Medium-firm drug-candidate library of cryptand-like structures on T7: Design and selection of strong binder for Hsp90

doi: 10.1039/D0OB01855D

Organic & Biomolecular Chemistry

Accepted Manuscript

This article can be cited before page numbers have been issued, to do this please use: K. Mochizuki, L. Matsukura, Y. Ito, N. Miyashita and M. Taki, *Org. Biomol. Chem.*, 2020, DOI: 10.1039/D0OB01855D.

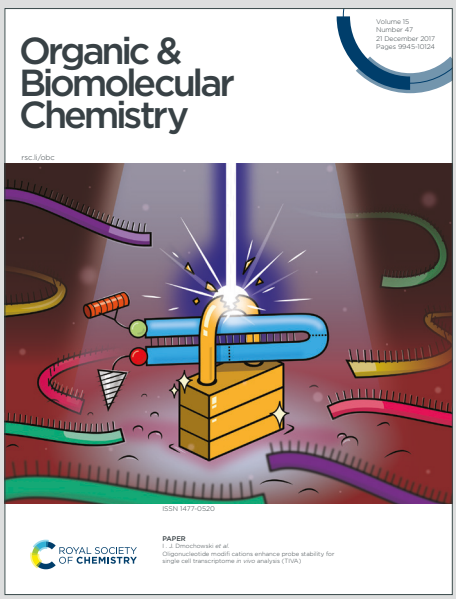

ROYAL SOCIETY OF CHEMISTRY

rsc.li/obc

View Article Online
DOI: 10.1039/D0OB01855D

COMMUNICATION

Medium-firm drug-candidate library of cryptand-like structures on T7: Design and selection of strong binder for Hsp90

Received 00th January 20xx,
Accepted 00th January 20xx

DOI: 10.1039/x0xx00000x

Kazuto Mochizuki,‡[a]§ Lisa Matsukura,‡[b] Yuji Ito,[c] Naoyuki Miyashita*[b] and Masumi Taki *[a]

We designed and synthesized a medium-firm drug-candidate library of cryptand-like structures possessing randomized peptide linker on bacteriophage T7. From the macrocyclic library with 10^9 diversity, we obtained a binder toward a cancer-related protein (Hsp90) with an antibody-like strong affinity (K_D = 62 nM) and the binding was driven by the enthalpy. The selected supramolecule inhibited Hsp90 activity by site-specific binding outside of the well-known ATP-binding pocket on the N-terminal domain (NTD).

Macrocycles, such as cyclophanes,[1, 2] calixarenes,[3-6] porphyrinoids,[7, 8] cyclodextrines,[9, 10] cucurbiturils,[11, 12] and so many other types[15] including their hybrids,[16-18] have been utilized to recognize specific molecules especially in supramolecular host-guest chemistry[19, 20] field. Recently, their applications are broadened to the fields of polymer/materials chemistry,[10, 20, 21] nanotechnology,[22] bio-oriented chemistry,[5, 10, 17, 23] optic sensors,[24] and more. Among them, specific recognition of biopolymers, such as peptides or proteins, by the supramolecular ligands[6, 25-27] as potential targeted-drugs are attracting attentions, and yet in a premature stage.[27, 28]

Meanwhile, we postulate that the limited utilization of such macrocyclic supramolecular ligands for the biomolecule recognition arises from lack of structural diversities. For example, synthesizable library size of azacrown ether derivatives is usually up to 10^1 order.[29, 30] To expand the diversity, we have previously demonstrated the first example to construct a library of azacrown-ether-like structures with vast diversity of 10^9 on T7 phage via the gp10 based-thioetherification (10BASE$_d$-T[31]), and successfully found a specific binder toward a cancer-related protein (*i.e.,* Heat shock protein 90 N-terminal domain; Hsp90NTD).[14] Nevertheless, one of the major drawbacks of the library is that strong binders as antibody substitutes can never be obtained. Judging from circular dichroism (CD) spectroscopy and isothermal titration calorimetry (ITC) measurement, whole structure of the obtained binder seems too flexible and unfavourable entropy loss happens upon the Hsp90 binding. The artificial binder should have possessed more rigidity[32] or more enthalpy compensation over the entropy penalty,[33] like natural antibodies or cyclic peptides do.

To increase the affinity with retaining the balance, here we generated a medium-firm [34, 35] drug-candidate library of cryptand[36, 37]-like structures instead of the library of crown-like structures as shown in Fig. 1, and successfully selected a Hsp90NTD binder with an antibody-like[38] strong affinity. The

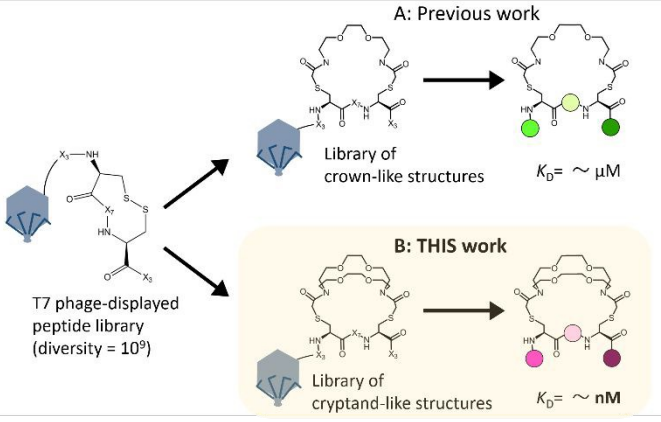

Fig. 1 Two types of macrocyclic libraries on bacteriophage T7 for finding Hsp90 binders. The starting peptide library on phage was the very same; X represents randomized amino acid. (A) Previous work: a selected crown-like binder possesses a weak affinity for Hsp90NTD.[14] (B) This work: a cryptand-like binder possessed a high affinity.

[a] *Department of Engineering Science, Bioscience and Technology Program, The Graduate School of Informatics and Engineering, The University of Electro-Communications (UEC), 1-5-1 Chofugaoka, Chofu, Tokyo 182-8585, Japan. Tel: +81-42-443-5980; E-mail: taki@pc.uec.ac.jp (M.T.)*
[b] *Department of Biological Systems Engineering, Graduate School of Biology-Oriented Science and Technology, KINDAI University, 930 Nishimitani, Kinokawa, Wakayama 649-6493, Japan. Tel: +91-736-77-3888, E-mail: miya@waka.kindai.ac.jp (N.M.).*
[c] *Department of Chemistry and Bioscience, Graduate School of Science and Engineering, Kagoshima University, 1-21-35 Korimoto, Kagoshima, Kagoshima 890-0065, Japan.*

† Electronic Supplementary Information (ESI) available: [details of any supplementary information available should be included here]. See DOI: 10.1039/x0xx00000x

‡ These authors equally contributed to the work.

§ Current affiliation: Tokyo Metropolitan Industrial Technology Research Institute, 2-4-10 Aomi, Koto-ku, Tokyo 135-0064, Japan.

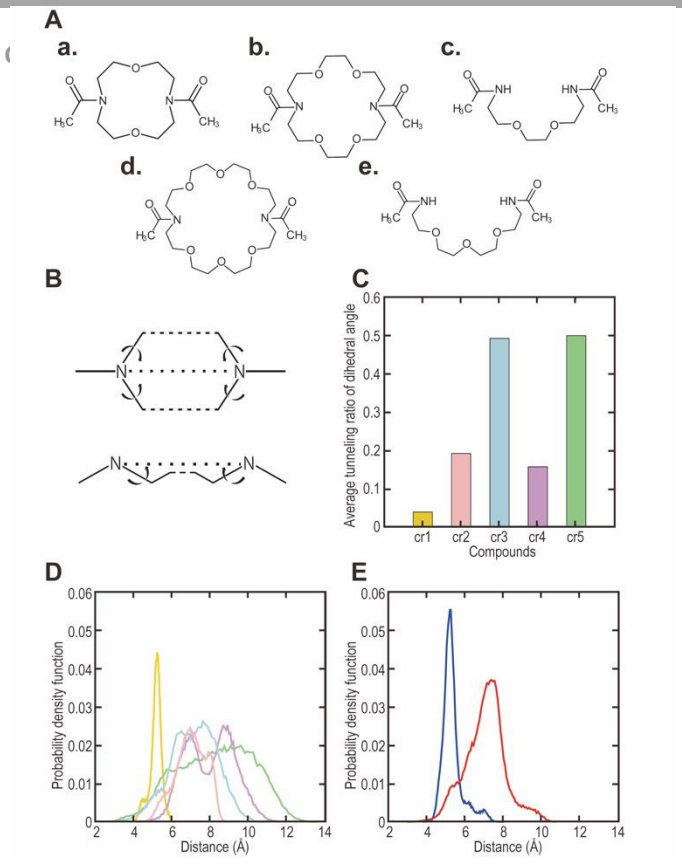

Fig. 2 Computer designing of a core structure possessing well-balanced flexibility. (A) (a) to (e) are core candidates (*i.e.*, precursors; cr1, cr2, cr3, cr4, and cr5, respectively) for synthesizing cryptand/crown-like macrocyclic libraries. (B) A schematic view of the dihedral angles to evaluate the fluctuation of the candidate compounds. (C) Averaged tunnelling ratio of the dihedral angle for the candidate compounds. (D) Probability density function of the distance between nitrogen-nitrogen atoms (N-N) in the core candidates. Yellow, pink, cyan, magenta, and green indicate cr1, cr2, cr3, cr4, and cr5, respectively. (E) Probability density function of the distance between N-N in the selected cryptand-like Hsp90NTD binder (blue) or crown-like binder[14] (red).

advantages of using the cryptand library over the crown one are: 1) more constrained cryptand scaffold would minimize conformational entropy loss upon the binding.[39] 2) favourable enthalpy contribution would be expected by increasing the numbers of hydrogen-bond acceptors (*i.e.,* ether oxygen atoms on the macrocycle), when their geometries are optimized[32] to fit to the basic protein (*i.e.,* Hsp90NTD possessing many hydrogen-bond donors). To design a core structure of the artificial macrocycle, we estimated the flexibility of several core candidates from long-time molecular dynamics (MD) simulations (Fig. 2).[40, 41] Two out of the three candidates of cryptand-precursors possessed well-balanced flexibility (*i.e.,* cr2 and cr4 in Fig. 2C), and the average distances between nitrogen-nitrogen atoms of these cryptand-precursors were similar to these of the corresponding crown-precursors (Fig. 2D). In addition to the flexibility and geometric homogeneity balance, cr2 has been known to recognize side-chain of the basic amino acids (*i.e.,* lysine and arginine).[25, 42] These points indicate that cr2 precursor is the most appropriate to the Hsp90 binder.

In advance to perform the library construction, we confirmed the expected cyclization using a T7 phage displaying

View Article Online
DOI: 10.1039/D0OB01855D

a model peptide (-GSRVS-C-GGRDRPG-C-LSV); we conjugated both amino ends of 1,10-diaza-18-crown-6 ether and designated two cysteines (Cys) on the peptide. After the cyclization against the model phage, total proteins were subjected to sodium dodecyl sulfate-polyacrylamide gel electrophoresis (SDS-PAGE) followed by coomassie brilliant blue (CBB) staining. The model-peptide-fused T7 capsid protein (*i.e.,* gp10) was excised from the gel, and then digested with trypsin. The resulting peptide fragments were analysed by liquid chromatography-tandem mass spectrometry (LC-MS/MS).[14] The *m/z* values of a parent ion from MS and those of the cyclized peptide from MS/MS indicate that Cys in the model phage-displayed peptide were position-specifically conjugated with the diazacrown derivative to form the macrocyclic cryptand structure (Fig. S1, †ESI).

Next, we constructed the library of cryptand-like structures and performed a selection against Hsp90NTD. From a phage-displayed peptide library (-SGGG-X_3-C-X_7-C-X_3; where X represents any amino acids),[31, 43] the library of cryptand-like structures was constructed in the same way via the 10BASE$_d$-T (Fig. 1B). Seven rounds of biopanning were performed against biotinylated-Hsp90NTD fused with glutathione-S-transferase (GST), and enrichment of Hsp90NTD binders was assessed by enzyme-linked immunosorbent assay (ELISA) as shown in Fig. 3B. After the biopanning, the selected cryptand on T7 phage polyclone showed the strongest binding to Hsp90NTD, whereas ones lacking the cryptand structure did not (Fig. S2A, †ESI). Among 9 monoclones of randomly chosen T7 phage from the polyclone, 6 clones had the same peptide sequence, QWV-C-LNPWLSI-C-RA (Cys were cyclized with the diazacrown derivative) (Fig. S2B, †ESI). The sequence was different from

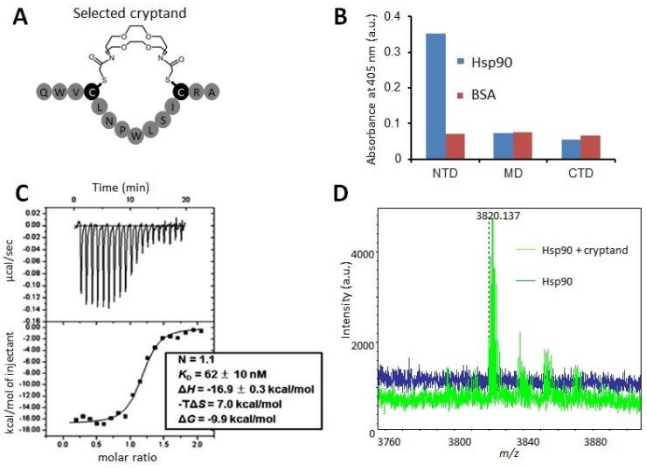

Fig. 3 (A) Structure of the selected cryptand-like binder. The azacrown moiety and N-terminal lariat (*i.e.,* QW) was essential for Hsp90NTD-specific strong binding. (B) Cryptand-binding domain on Hsp90 was identified by enzyme-linked immunosorbent assay (ELISA). N-terminal (NTD), middle (MD), and C-terminal (CTD) domains of Hsp90 fused with glutathione-S-transferase (GST) were independently assayed against the selected cryptand on phage. Bovine serum albumin (BSA; target-unrelated protein) was served as a negative control. (C) Isothermal titration calorimetry (ITC) profiles of titrations of the selected cryptand against GST-Hsp90NTD. *N*: number of binding sites, K_D: dissociation constant, *ΔH*: enthalpy change, *ΔS*: entropy change, *T*: temperature (*i.e.*, 298 K), *ΔG*: free energy change. (D) Identification of the cryptand binding site on Hsp90NTD by mass spectrometry (MS). A crosslinked cryptand-Hsp90NTD was digested with trypsin, and the conjugated fragment (*i.e.*, Hsp90 + cryptand; green line) was analysed by MALDI−TOF MS. A mock crosslinking was also performed in the absence of cryptand (*i.e.*, Hsp90; blue line). The new fragment was observed only when both GST-Hsp90NTD and the selected cryptand were present.

View Article Online
DOI: 10.1039/D0OB01855D

what is discovered from the library of crown-like structures,[14] although the starting phage-displayed peptide library is the very same (Fig. 1A). This suggests that the different oligoethylene glycol moieties may affect the geometries of the whole macrocycle structures constructed from the starting library, to generate independent libraries.

To determine an affinity of the Hsp90NTD-binding cryptand, we chemically synthesized the selected peptide sequence followed by cyclization with the azacrown derivative. ITC measurement was performed to obtain the dissociation constant (K_D) as well as thermodynamic parameters (Fig. 3C). The selected cryptand possessed a high affinity toward GST-Hsp90NTD with the K_D value of 62 ± 10 nM, whereas the selected peptide lacking the cryptand structure did not (Fig. S6, †ESI). This indicates that both structures of the azacrown moiety and the rest of the peptide are essential for the Hsp90-specific strong binding. Also, an expected larger negative enthalpy change (ΔH = -16.9 ± 0.3 kcal/mol), compared to our previous crown-like binder (-13.7 ± 1.6 kcal/mol),[14] was observed, suggesting that numbers of hydrogen bonds and van der Waals interactions may contribute to the favourable binding between the selected cryptand and Hsp90NTD. To investigate the secondary structure of the macrocycle, we measured circular dichroism (CD) spectra before and after the cyclization of the selected peptide (Fig. S3, †ESI). They were almost superimposable each other, and indicated that the selected peptide possessed a β-turn structure regardless of the azacrown moiety. Taken into account of the rigidity of the β-turn, we tentatively think that a slight unfavourable entropy change (-TΔS = +7.0 kcal/mol) could arise from the enthalpy penalty associated with desolvation of polar groups (*i.e.,* entropy-enthalpy compensation),[32] rather than from the conformational entropy loss deduced from our previous crown-like binder[14] possessing more flexible core structure. In the MD simulations, it was shown the fluctuation in the cryptand-like binder was less than that in the crown-like binder (Fig. 2E). Moreover, the interaction between Trp_2 (W_2) and Arg_{13} (R_{13}) was frequently found during a long-time MD simulation of the cryptand-like binder (Fig. S12D). Importance of W_2 at the N-terminal lariat for the strong binding was also indicated experimentally; a Q_1W_2-deleted cryptand at the same molar concentration showed less intense saturation transfer difference (STD) signals[44] in proton nuclear magnetic resonance (^{1}H NMR) spectroscopy (Fig. S4B, †ESI), and increased about 10^3 order of the dissociation constant in ITC measurement (Fig. S6, †ESI). To sum up, appropriate electrostatic / hydrophobic effects arose from whole regions (*i.e.*, azacrown and peptide moieties) of the cryptand to afford a strong supramolecular interaction toward Hsp90NTD.

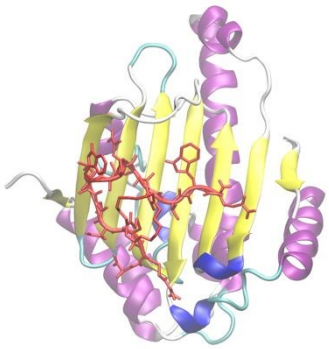

Fig. 4 Docking model of cryptand and Hsp90NTD deduced from both experimental and computational results. Yellow and purple indicate β-sheets and α-helices.[13] The cryptand-like binder, which is indicated by red colour, bound to the β-sheets region.

Using the selected cryptand, we performed more detailed structural analysis including binding-site determination on Hsp90NTD. A fluorescence polarization (FP) competition assay using fluorescein-5-isothiocyanate labelled geldanamycin (GA-FITC), which binds to the ATP-binding pocket on Hsp90NTD, indicated that the selected cryptand did not compete with GA-FITC (Fig. S5, †ESI). This means that the cryptand bound outside of the ATP-binding pocket unlike most of the reported Hsp90NTD inhibitors.[45, 46] To determine the binding site, the cryptand on Hsp90NTD was covalently conjugated with a bifunctional crosslinker (succinimidyl-ester diazirine; SDA). After the hetero-crosslinking, it was digested with trypsin and the crosslinked fragment was analysed by matrix-assisted laser desorption/ionization time-of-flight mass spectrometry (MALDI–TOF MS; Fig. 3D). From the *m/z* value of a newly appeared fragment, the binding site was deduced to be the β-sheets region in Hsp90NTD, which was consistent with the FP competition assay above. Also, the binding site was determined by a long-time MD simulation between the selected cryptand and Hsp90NTD,[47] followed by a docking simulation by AutoDock Vina.[48] As shown in Fig. 4, a most reasonable structure was obtained, which was again consistent with all of the experimental results. The β-sheets region of Hsp90NTD, in which the cryptand bound, would possibly be a novel drug targeting site, because Hsp90 chaperone machinery was inhibited upon the binding (Fig. S7).[49]

Conclusions

In conclusion, we demonstrated the first example to design and construct a library of unclosed-cryptand[36] with two lariat arms using T7-phage display system, and successfully selected a strong Hsp90NTD-specific binder. It is emphasized that such discovery of a functional supramolecular ligand was attained by an ensemble of MD-simulation-assisted rational design of the artificial macrocyclic moiety and genetically-encoded random peptide structure.

Since there are sophisticated alternative library-construction systems for obtaining macrocyclic targeted drugs[50, 51] with strong affinities,[52-55] we think that using such artificial moiety just for the target recognition is not the final achievement. More advanced artificial functionalization on the moiety, such as the addition of catalytic activity (*e.g.,* proteolytic actions by complexation with metals[56, 57]), fluorescent chemosensor,[58] optochemical property,[59] or cell permeability,[60-62] would be one of the future directions of the bio-oriented supramolecules possessing expanded diversities.

This work was supported by JSPS KAKENHI Grant Numbers 17K05925, 17J10365, and 17K00421 to M.T, K.M, and N.M, respectively. Simulation studies used computational resources of MOMO provided by BOST Computer Centre, KINDAI University (N.M, L.M), and TSUBAME3.0 provided by Tokyo Institute of Technology through TSUBAME Encouragement Program for Young/Female Users (Project ID: 19IJ0037) (L.M). We are grateful to Dr. F.U. Hartl for providing plasmids, Dr. Y. Minami for providing proteins, Dr. K. Ikebukuro and Dr. J. Lee for use of ITC instrument installed by the Low-Carbon Research Network Japan (LCnet), Dr. S. Hosoya (TMDU), and Dr. S. Ohdan for technical assistance and valuable suggestions.

Conflicts of interest

There are no conflicts to declare.

Notes and references

1. Z. Hassan, E. Spuling, D. M. Knoll and S. Brase, *Angew. Chem. Int. Ed. Engl.*, 2020, **59**, 2156-2170.
2. J. Nishimura, Y. Nakamura, Y. Hayashida and T. Kudo, *Acc. Chem. Res.*, 2000, **33**, 679-686.
3. L. Troian-Gautier, A. Mattiuzzi, O. Reinaud, C. Lagrost and I. Jabin, *Org. Biomol. Chem.*, 2020, **18**, 3624-3637.
4. M. X. Wang, *Acc. Chem. Res.*, 2012, **45**, 182-195.
5. S. B. Nimse and T. Kim, *Chem. Soc. Rev.*, 2013, **42**, 366-386.
6. A. M. Doolan, M. L. Rennie and P. B. Crowley, *Chemistry*, 2018, **24**, 984-991.
7. W. Stawski, M. Kijewska and M. Pawlicki, *Chem. Asian. J.*, 2020, **15**, 8-20.
8. R. S. Czernuszewicz, V. Mody, A. Czader, M. Galezowski and D. T. Gryko, *J. Am. Chem. Soc.*, 2009, **131**, 14214-14215.
9. Y. M. Zhang, Y. H. Liu and Y. Liu, *Adv. Mater.*, 2020, **32**, e1806158.
10. B. Kost, M. Brzezinski, M. Socka, M. Basko and T. Biela, *Molecules*, 2020, **25**, 3404.
11. K. M. Park, M. Y. Hur, S. K. Ghosh, D. R. Boraste, S. Kim and K. Kim, *Chem. Commun.*, 2019, **55**, 10654-10664.
12. L. Isaacs, *Acc. Chem. Res.*, 2014, **47**, 2052-2062.
13. W. Humphrey, A. Dalke and K. Schulten, *J. Mol. Graph. Model.*, 1996, **14**, 33-38.
14. K. Fukunaga, T. Hatanaka, Y. Ito, M. Minami and M. Taki, *Chem. Commun.*, 2014, **50**, 3921-3923.
15. L. P. Yang and W. Jiang, *Angew. Chem. Int. Ed. Engl.*, 2020, **59**, 15794-15796.
16. E. Pazos, P. Novo, C. Peinador, A. E. Kaifer and M. D. Garcia, *Angew. Chem. Int. Ed. Engl.*, 2019, **58**, 403-416.
17. I. M. Mavridis and K. Yannakopoulou, *J. Med. Chem.*, 2020, **63**, 3391-3424.
18. X. Wu, Y. Chen, Q. Yu, F. Q. Li and Y. Liu, *Chem. Commun.*, 2019, **55**, 4343-4346.
19. A. Blanco-Gomez, P. Corton, L. Barravecchia, I. Neira, E. Pazos, C. Peinador and M. D. Garcia, *Chem. Soc. Rev.*, 2020, **49**, 3834-3862.
20. S. Dong, B. Zheng, F. Wang and F. Huang, *Acc. Chem. Res.*, 2014, **47**, 1982-1994.
21. K. Jie, Y. Zhou, E. Li and F. Huang, *Acc. Chem. Res.*, 2018, **51**, 2064-2072.
22. V. Montes-Garcia, J. Perez-Juste, I. Pastoriza-Santos and L. M. Liz-Marzan, *Chemistry*, 2014, **20**, 10874-10883.
23. C. C. Lee, M. Maestre-Reyna, K. C. Hsu, H. C. Wang, C. I. Liu, W. Y. Jeng, L. L. Lin, R. Wood, C. C. Chou, J. M. Yang and A. H. J. Wang, *Angew. Chem. Int. Ed. Engl.*, 2014, **53**, 13054-13058.
24. M. Qi, N. M. Y. Zhang, K. Li, S. C. Tjin and L. Wei, *Sensors*, 2020, **20**, 3266.
25. S. X. Fa and Y. Zhao, *Chem. Mater.*, 2019, **31**, 4889-4896.
26. Y. Zhao, *Chemistry*, 2018, **24**, 14001-14009.
27. S. van Dun, C. Ottmann, L. G. Milroy and L. Brunsveld, *J. Am. Chem. Soc.*, 2017, **139**, 13960-13968.
28. T. Yokoyama and M. Mizuguchi, *J. Med. Chem.*, 2019, **62**, 2076-2082.
29. Y. Luo, G. Ouyang, Y. Tang, Y. M. He and Q. H. Fan, *J. Org. Chem.*, 2020, **85**, 8176-8184.
30. G. Farruggia, S. Iotti, M. Lombardo, C. Marraccini, D. Petruzziello, L. Prodi, M. Sgarzi, C. Trombini and N. Zaccheroni, *J. Org. Chem.*, 2010, **75**, 6275-6278.
31. K. Fukunaga, T. Hatanaka, Y. Ito and M. Taki, *Mol. Biosyst.*, 2013, **9**, 2988-2991.
32. E. Freire, *Drug Discovery Today*, 2008, **13**, 869-874.
33. B. Zhao, P. Xu, L. Jiang, B. Paaske, T. Kromann-Hansen, J. K. Jensen, H. P. Sorensen, Z. Liu, J. T. Nielsen, A. Christensen, M. Hosseini, K. K. Sorensen, N. C. Nielsen, K. J. Jensen, M. Huang and P. A. Andreasen, *PLoS One*, 2014, **9**, e115872.
34. B. C. Doak, J. Zheng, D. Dobritzsch and J. Kihlberg, *J. Med. Chem.*, 2016, **59**, 2312-2327.
35. F. Giordanetto and J. Kihlberg, *J. Med. Chem.*, 2014, **57**, 278-295.
36. K. Dabrowa, M. Pawlak, P. Duszewski and J. Jurczak, *Org. Lett.*, 2012, **14**, 6298-6301.
37. Y. Han, Y. Jiang and C. F. Chen, *Tetrahedron*, 2015, **71**, 503-522.
38. R. Ahirwar, S. Nahar, S. Aggarwal, S. Ramachandran, S. Maiti and P. Nahar, *Sci. Rep.*, 2016, **6**, 21285.
39. E. M. Driggers, S. P. Hale, J. Lee and N. K. Terrett, *Nat. Rev. Drug Discov.*, 2008, **7**, 608-624.
40. H. J. C. Berendsen, D. Vanderspoel and R. Vandrunen, *Comp. Phys. Commun.*, 1995, **91**, 43-56.
41. J. M. Wang, R. M. Wolf, J. W. Caldwell, P. A. Kollman and D. A. Case, *J. Comp. Chem.*, 2004, **25**, 1157-1174.
42. S. Fa and Y. Zhao, *Chem. Mater.*, 2017, **29**, 9284-9291.
43. T. Hatanaka, S. Ohzono, M. Park, K. Sakamoto, S. Tsukamoto, R. Sugita, H. Ishitobi, T. Mori, O. Ito, K. Sorajo, K. Sugimura, S. Ham and Y. Ito, *J. Biol. Chem.*, 2012, **287**, 43126-43136.
44. A. Viegas, J. Manso, F. L. Nobrega and E. J. Cabrita, *J. Chem. Educ.*, 2011, **88**, 990-994.
45. L. Li, L. Wang, Q. D. You and X. L. Xu, *J. Med. Chem.*, 2020, **63**, 1798-1822.
46. T. Ueda, T. Tamura and I. Hamachi, *Biochemistry*, 2020, **59**, 179-182.
47. R. Galindo-Murillo, J. C. Robertson, M. Zgarbova, J. Sponer, M. Otyepka, P. Jurecka and T. E. Cheatham, *J. Chem. Theo. Comp.*, 2016, **12**, 4114-4127.

View Article Online
DOI: 10.1039/D0OB01855D

48. O. Trott and A. J. Olson, *J. Comp. Chem.*, 2010, **31**, 455-461.
49. J. Davenport, M. Balch, L. Galam, A. Girgis, J. Hall, B. S. Blagg and R. L. Matts, *Biology*, 2014, **3**, 101-138.
50. P. G. Dougherty, Z. Q. Qian and D. H. Pei, *Biochem. J.*, 2017, **474**, 1109-1125.
51. T. Passioura, *Biochemistry*, 2020, **59**, 139-145.
52. T. Anananuchatkul, I. V. Chang, T. Miki, H. Tsutsumi and H. Mihara, *ACS Omega*, 2020, **5**, 5666-5674.
53. S. Chen, I. Rentero Rebollo, S. A. Buth, J. Morales-Sanfrutos, J. Touati, P. G. Leiman and C. Heinis, *J. Am. Chem. Soc.*, 2013, **135**, 6562-6569.
54. A. A. Vinogradov, Y. Z. Yin and H. Suga, *J. Am. Chem. Soc.*, 2019, **141**, 4167-4181.
55. C. Heinis and G. Winter, *Curr. Opin. Chem. Biol.*, 2015, **26**, 89-98.
56. S. Mahesh, K. C. Tang and M. Raj, *Molecules*, 2018, **23**.
57. J. Suh, *Asian J. Org. Chem.*, 2014, **3**, 18-32.
58. M. A. Beatty, A. J. Selinger, Y. Li and F. Hof, *J. Am. Chem. Soc.*, 2019, **141**, 16763-16771.
59. M. R. Jafari, H. Yu, J. M. Wickware, Y. S. Lin and R. Derda, *Org. Biomol. Chem.*, 2018, **16**, 7588-7594.
60. J. Mosquera, I. Garcia and L. M. Liz-Marzan, *Acc. Chem. Res.*, 2018, **51**, 2305-2313.
61. J. Rodriguez, J. Mosquera, J. R. Couceiro, J. R. Nitschke, M. E. Vazquez and J. L. Mascarenas, *J. Am. Chem. Soc.*, 2017, **139**, 55-58.
62. H. Fernandez-Caro, I. Lostale-Seijo, M. Martinez-Calvo, J. Mosquera, J. L. Mascarenas and J. Montenegro, *Chem. Sci.*, 2019, **10**, 8930-8938.

View Article Online
DOI: 10.1039/D0OB01855D

Table of Contents:

We designed and synthesized a library of cryptand-like structures on T7 phage; a strong binder for a cancer-related protein was selected from the library.